SARS-like WIV1-CoV poised for human emergence

Vineet D. Menachery[a], Boyd L. Yount Jr.[a], Amy C. Sims[a], Kari Debbink[a,b], Sudhakar S. Agnihothram[c], Lisa E. Gralinski[a], Rachel L. Graham[a], Trevor Scobey[a], Jessica A. Plante[a], Scott R. Royal[a], Jesica Swanstrom[a], Timothy P. Sheahan[a], Raymond J. Pickles[c,d], Davide Corti[e,f,g], Scott H. Randell[d], Antonio Lanzavecchia[e,f], Wayne A. Marasco[h], and Ralph S. Baric[a,c,1]

[a]Department of Epidemiology, University of North Carolina at Chapel Hill, Chapel Hill, NC 27599; [b]Department of Microbiology and Immunology, University of North Carolina at Chapel Hill, Chapel Hill, NC 27599; [c]Division of Microbiology, National Center for Toxicological Research, Food and Drug Administration, Jefferson, AR 72079; [d]Department of Cell Biology and Physiology and Marsico Lung Institute/Cystic Fibrosis Center, University of North Carolina at Chapel Hill, Chapel Hill, NC 27599; [e]Institute for Research in Biomedicine, Bellinzona, Switzerland; [f]Institute of Microbiology, Eidgenössische Technische Hochschule Zurich, Zurich, Switzerland; [g]Humabs BioMed SA, Bellinzona, Switzerland; and [h]Department of Cancer Immunology and AIDS, Dana-Farber Cancer Institute–Department of Medicine, Harvard Medical School, Boston MA 02215

Edited by Peter Palese, Icahn School of Medicine at Mount Sinai, New York, NY, and approved January 6, 2016 (received for review September 4, 2015)

Outbreaks from zoonotic sources represent a threat to both human disease as well as the global economy. Despite a wealth of metagenomics studies, methods to leverage these datasets to identify future threats are underdeveloped. In this study, we describe an approach that combines existing metagenomics data with reverse genetics to engineer reagents to evaluate emergence and pathogenic potential of circulating zoonotic viruses. Focusing on the severe acute respiratory syndrome (SARS)-like viruses, the results indicate that the WIV1-coronavirus (CoV) cluster has the ability to directly infect and may undergo limited transmission in human populations. However, in vivo attenuation suggests additional adaptation is required for epidemic disease. Importantly, available SARS monoclonal antibodies offered success in limiting viral infection absent from available vaccine approaches. Together, the data highlight the utility of a platform to identify and prioritize prepandemic strains harbored in animal reservoirs and document the threat posed by WIV1-CoV for emergence in human populations.

SARS | CoV | emergence | Spike | WIV1

Although previously associated with upper respiratory infections, the emergence of severe acute respiratory coronavirus (SARS-CoV) in 2002–2003, and more recently, Middle East respiratory syndrome (MERS)-CoV underscores the threat of cross-species transmission leading to virulent pandemic viral infections (1, 2). Whereas prevailing research suggests that SARS-CoV emerged from viruses in the Chinese horseshoe bat, identifying a progenitor strain that used human angiotensin converting enzyme 2 (*ACE2*) had proven elusive (3, 4). However, recent metagenomics studies isolated several SARS-like virus sequences that share ≥90% genome-wide homology and represented the closest sequences to the epidemic strains (5, 6). Importantly, researchers also isolated replication competent virus; WIV1-CoV, part of the Rs3306 cluster, could use ACE2 orthologs and mediated low-level replication in human cells (5). Overall, the evidence indicates that SARS-CoV likely emerged from Chinese horseshoe bats and that similar viruses are still harbored in these populations.

The identification of WIV1-CoV and its capacity to use ACE2 orthologs offers a warning for possible reemergence and provides an opportunity to prepare for a future CoV outbreak. To achieve this goal, a new platform is required to translate metagenomics findings; the approach must generate critical diagnostic reagents, define emergence potential of novel strains, and determine efficacy of current therapeutics. Building on this premise, we developed a framework to examine circulating CoVs using reverse genetic systems to construct full-length and chimeric viruses. The results indicate that viruses using WIV1-CoV spike are poised to emerge in human populations due to efficient replication in primary human airway epithelial cell cultures. However, additional adaptation, potentially independent of the spike protein receptor-binding domain, is required for pathogenesis and epidemic disease. Importantly, monoclonal antibody strategies against SARS were effective against WIV1-CoV spike unlike available vaccine approaches. Together, the results highlight the utility of developing platforms to evaluate circulating zoonotic viruses as threats for future emergence and epidemic potential.

Results

The discovery of SARS-like virus clusters that bridge the gap between the epidemic strains and related precursor CoV strain HKU3 virus provided the best evidence for emergence of SARS-CoV from Chinese horseshoe bats (5). Comparing the receptor binding domain (RBD), SARS-CoV Urbani and WIV1 share homology at 11 of the 14 contact residues with human ACE2 (Fig. 1*A*); importantly, the three amino acid changes represent relatively conservative substitution not predicted to ablate binding (Fig. 1*B*). Therefore, exploring WIV1 strains allows examination of emergence, pathogenesis potential, and adaptation requirements. Using the SARS-CoV infectious clone as a template (7), we designed and synthesized a full-length infectious clone of WIV1-CoV consisting of six plasmids that could be enzymatically cut, ligated together, and electroporated into cells to rescue replication competent progeny virions (Fig. S1*A*). In addition to the full-length clone, we also produced WIV1-CoV

Significance

The emergence of severe acute respiratory syndrome coronavirus (SARS-CoV) and Middle East respiratory syndrome (MERS)-CoV highlights the continued risk of cross-species transmission leading to epidemic disease. This manuscript describes efforts to extend surveillance beyond sequence analysis, constructing chimeric and full-length zoonotic coronaviruses to evaluate emergence potential. Focusing on SARS-like virus sequences isolated from Chinese horseshoe bats, the results indicate a significant threat posed by WIV1-CoV. Both full-length and chimeric WIV1-CoV readily replicated efficiently in human airway cultures and in vivo, suggesting capability of direct transmission to humans. In addition, while monoclonal antibody treatments prove effective, the SARS-based vaccine approach failed to confer protection. Together, the study indicates an ongoing threat posed by WIV1-related viruses and the need for continued study and surveillance.

Author contributions: V.D.M., B.L.Y., and R.S.B. designed research; V.D.M., B.L.Y., A.C.S., S.S.A., L.E.G., T.S., J.A.P., S.R.R., J.S., and T.P.S. performed research; V.D.M., B.L.Y., R.J.P., D.C., S.H.R., A.L., and W.A.M. contributed new reagents/analytic tools; V.D.M., A.C.S., K.D., R.L.G., and R.S.B. analyzed data; and V.D.M. and R.S.B. wrote the paper.

The authors declare no conflict of interest.

This article is a PNAS Direct Submission.

Freely available online through the PNAS open access option.

See Commentary on page 2812.

[1]To whom correspondence should be addressed. Email: rbaric@email.unc.edu.

This article contains supporting information online at www.pnas.org/lookup/suppl/doi:10.1073/pnas.1517719113/-/DCSupplemental.

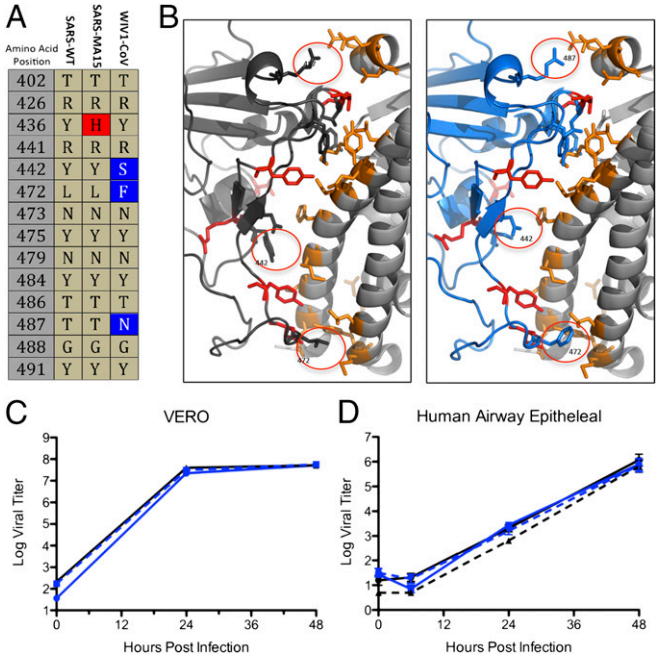

Fig. 1. Full-length and chimeric WIV1 infectious clones produce viruses that replicate in primary human airway epithelial cell cultures. (*A*) Spike amino acid residues that interact directly with human ACE2 from SARS-CoV, SARS-MA15, and WIV1-CoV spike proteins. Residue changes are highlighted by color. (*B*) Interaction between S1 domain of SARS-Urbani spike (black) and WIV1 spike (blue) with human ACE2 (gray). Contact residues highlighted with consensus amino acids (red) and differences (circled) between SARS and WIV1 spike proteins; human ACE2 contact residues are also highlighted (orange). (*C*) Viral replication of WIV1-CoV (blue), WIV1-MA15 (blue hatched), and SARS-CoV Urbani (black) following infection of Vero cells at a multiplicity of infection (MOI) of 0.01. (*D*) Well-differentiated air–liquid interface primary human airway epithelial cell cultures were infected with SARS-CoV Urbani (black), SARS-CoV MA15 (black hatched), WIV1-MA15 (blue-white hatched), and WIV-CoV (blue) at (*E*) MOI of 0.01 in cells from the same donor at an MOI of 0.01. Samples were collected at individual time points with biological replicates ($n = 3$) for all experiments for both *C* and *D*.

chimeric virus that replaced the SARS spike with the WIV1 spike within the mouse-adapted backbone (WIV1-MA15, Fig. S1*B*). WIV1-MA15 incorporates the original binding and entry capabilities of WIV1-CoV, but maintains the backbone changes to mouse-adapted SARS-CoV. Importantly, WIV1-MA15 does not incorporate the Y436H mutation in spike that is required for SARS-MA15 pathogenesis (8). Following electroporation into Vero cells, robust stock titers were recovered from both chimeric WIV1-MA15 and WIV1-CoV. To confirm growth kinetics and replication, Vero cells were infected with SARS-CoV Urbani, WIV1-MA15, and WIV1-CoV (Fig. 1*C*); the results indicate similar replication kinetics and overall titers between the CoVs. However, Western blot analysis suggests potential differences in spike cleavage/processing of WIV1 and SARS-CoV spike proteins (Fig. S1*C*); the ratio of full-length to cleaved spike varied between SARS spikes (Urbani, 1.21; MA15, 1.44) and WIV1 (full length, 0.61; WIV1-MA15, 0.25) signaling possible variation in host proteolytic processing (Fig. S1*D*). Overall, the results indicate comparable viral replication, but possible biochemical differences in processing.

Replication in Primary Human Epithelial Cells. Next, we wanted to determine WIV-CoV replication potential in models of the human lung. Previous examination of WIV1-CoV recovered from bat samples demonstrated poor replication in A549 cells (5); however, replication of epidemic SARS-CoV is also poor in this cell type, potentially due to ACE2 expression levels (9). Therefore, well-differentiated primary human airway epithelial cell (HAE) air–liquid interface cultures were infected with WIV1-MA15, WIV1-CoV, SARS-CoV Urbani, or SARS-CoV MA15. At 24 and 48 h postinfection, both WIV1-MA15 and WIV1-CoV produce robust infection in HAE cultures equivalent to the epidemic strain and mouse-adapted strains (Fig. 1*D*). Together, the data demonstrate that the WIV1-CoV spike can mediate infection of human airway cultures with no significant adaptation required.

WIV1 Spike in Vivo. To extend analysis to pathogenesis, we next evaluated in vivo infection following WIV1-MA15 and WIV1-CoV challenge. Initial studies compared WIV1-MA15 to mouse-adapted SARS-CoV (MA15) to determine spike-dependent pathogenesis. Ten-week-old BALB/c mice were infected with 10^4 plaque forming units (pfu) of WIV1-MA15 or SARS-CoV MA15 and followed over a 4-d time course. As expected, animals infected with SARS-CoV MA15 experienced rapid weight loss and lethality by day 4 postinfection (Fig. 2*A* and Fig. S2*A*) (10). In contrast, WIV1-MA15 induced neither lethality nor notable changes in body weight, indicating limited disease in vivo. Viral titer in the lung also revealed reduced replication following WIV1-MA15 challenge compared with control (Fig. 2*B*). Similarly, lung antigen staining indicated distinct attenuation of the WIV1-MA15, with most staining occurring in the airways and absent from large regions of the lungs (Fig. S2 *B–D*). Together, these data indicate that WIV1 spike substitution does not program pathogenesis in the mouse-adapted SARS-CoV backbone.

Although chimeric studies suggest minimal pathogenesis potential for WIV1 spike, SARS-CoV Urbani spike within the mouse-adapted backbone yielded similar results (8). Therefore, we examined the full-length WIV1-CoV versus the epidemic SARS-CoV Urbani strain in vivo. Ten-week-old BALB/c mice

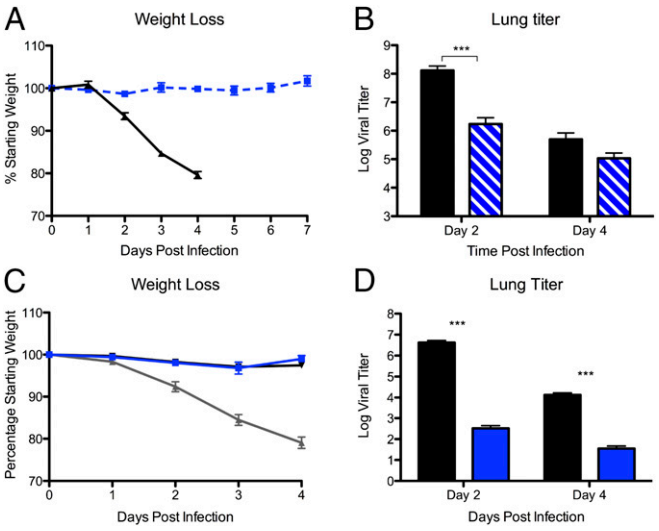

Fig. 2. Viruses using WIV1 spike attenuated relative to SARS spike in vivo. (*A* and *B*) Ten-week-old BALB/c mice were infected with 10^4 pfu of either SARS-CoV MA15 (black) or WIV1-MA15 (blue hatched) via the i.n. route and examined over a 7-d time course. (*A*) Weight loss ($n = 17$ for WIV1-MA15, $n = 9$ for SARS-CoV MA15) and (*B*) lung titer ($n = 3$ for MA15, $n = 4$ for WIV1-MA15. (*C* and *D*) Ten-week-old BALB/c mice were infected with 1×10^5 pfu of either SARS-CoV Urbani (black), WIV1-CoV (blue), or SARS-CoV MA15 (gray) and examined over a 4-d time course. (*C*) Weight loss ($n = 6$ for WIV1-CoV, $n = 6$ for SARS-CoV Urbani) and (*D*) lung titer ($n = 3$ for WIV1-CoV, $n = 3$ for SARS-CoV Urbani) were examined. For each bar graph, center value is representative of group mean and error bars are defined by SEM. *P* values based on two-tailed Student's *t* test of individual time points are marked as indicated: $***P < 0.001$.

were infected with 10^5 pfu of WIV1-CoV or SARS-CoV Urbani and followed over a 4-d time course. As expected, neither infection condition resulted in significant weight loss compared with MA15 (Fig. 2*C*). However, viral replication was significantly attenuated for WIV1-CoV compared with SARS-CoV Urbani (Fig. 2*D*); at both days 2 and 4 postinfection, WIV1-CoV titer was reduced nearly 10,000- and 1,000-fold, respectively. Similarly, only minor antigen staining was observed following WIV1-CoV infection, contrasting antigen staining throughout the parenchyma 2-d post–SARS-CoV Urbani infection (Fig. S2 *E* and *F*). Together, the data indicate significant attenuation of WIV1-CoV relative to the epidemic SARS-CoV in wild-type mice.

WIV1-CoV in Human ACE2 Expressing Mice. Whereas studies in wild-type mice provide insight into pathogenesis potential, the absence of clinical disease in the epidemic strains of SARS-CoV suggests that the mouse model may not be adequate to access human disease potential. To test a model more relevant to humans, we generated a mouse that expresses human ACE2 receptor under control of HFH4, a lung ciliated epithelial cell promoter (11). However, whereas robust expression was observed in the lung, other tissues including brain, liver, kidney, and gastrointestinal tract had varying levels of human ACE2 expression, indicating greater tissue distribution of HFH4-mediated expression than initially expected (Fig. S3*A*). In addition, examination of individual HFH4-ACE2–expressing progeny revealed the occasional absence of the human ACE2 gene, suggesting possible selection against human receptor (Fig. S3*B*). Therefore, PCR-positive, 10- to 20-wk-old HFH4-ACE2–expressing mice were infected with 10^5 pfu of WIV1-CoV or SARS-CoV Urbani and then followed for a 7-d time course to determine pathogenesis. The results indicated that WIV1-CoV infection was augmented, but remained attenuated relative to SARS-CoV Urbani in the presence of human *ACE2*. Following SARS-CoV Urbani challenge, HFH4-hACE2–expressing mice lost no weight, but then, experienced rapid weight loss and death between days 4 and 5 (Fig. 3*A* and Fig. S3*C*). In contrast, WIV1-CoV produce minimal changes in weight loss until late times where animals fell into distinct categories either losing less than or more than 10% of their body weight. Whereas day-2 lung titers were still attenuated relative to SARS-CoV Urbani, titers for WIV1-CoV were 100-fold higher in the presence of human ACE2 compared with wild-type BALB/c, with no similar augmentation observed with the epidemic SARS-CoV strain (Fig. 3*B*). Based on pilot studies and previous studies with ACE2 transgenic animals (12), mice experiencing rapid weight loss were predicted to have lethal encephalitis and were humanely killed and harvested for lung and brain titer if weight loss approached >20% of starting body weight. All HFH4-ACE2 mice infected with SARS-CoV Urbani lost >20% body weight and maintained robust replication in the lung and brain following infection (Fig. 3 *C* and *D*). Similarly, mice with >10% weight loss following WIV1-CoV infection produced robust viral replication in the brain, but significantly lower titers in the lung. In contrast, mice that maintained minimal weight loss (<10%) following WIV1-CoV infection after 7 d had minimal titers in both the lung and brain, suggesting a sufficient adaptive immune response was generated to clear virus and survive infection. Together, the data indicate that WIV1-CoV maintains attenuation relative to SARS-CoV Urbani despite the availability of human *ACE2*. In addition, augmented replication suggests that WIV1-CoV may bind the human ACE2 receptor more efficiently that the mouse ACE2, indicating potential inadequacies in the current mouse models of SARS pathogenesis.

Therapeutics Against WIV1 Emergence. Having established a potential threat based on replication in primary human cells and preference for the human ACE2 receptor in vivo, we next sought

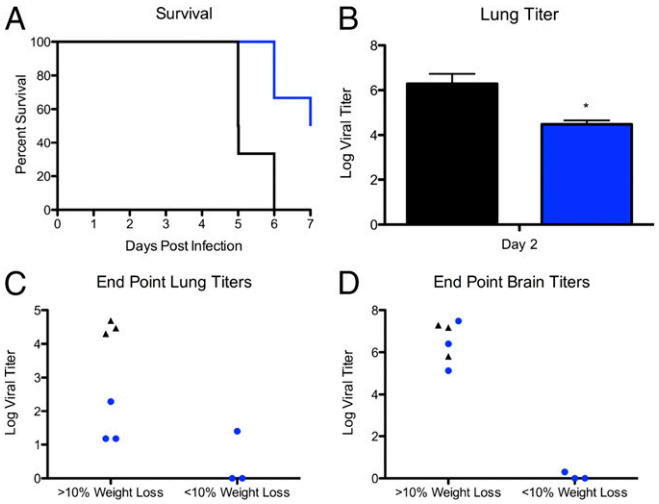

Fig. 3. WIV1-Cov still attenuated despite human ACE2 expression in vivo. (*A*) Ten- to twenty-week-old HFH4 ACE2-expressing mice were infected with 10^5 pfu of SARS-CoV Urbani (black) or WIV1-CoV (blue) and examined over a 7-d time course for (*A*) survival and (*B*) day-2 lung titer ($n = 3$ for WIV1-CoV, $n = 3$ for SARS-CoV Urbani). (*C* and *D*) Upon reaching thresholds for humane sacrifice (>20% weight loss) or 7 d postinfection (DPI), endpoint titers were determined in the (*C*) lung and (*D*) brain following infection. *P* values based on two-tailed Student's *t* test of individual time points are marked as indicated: $*P < 0.05$.

to determine if monoclonal antibody therapies could be used to lessen disease similar to ZMApp for Ebola (13). We first tested a SARS-CoV monoclonal derived via phage display and antibody escape (Fm6) (14) and found both wild-type SARS-CoV Urbani and WIV1-MA15 were strongly neutralized at low antibody concentrations (Fig. 4*A*). Similarly, a panel of monoclonal antibodies derived from B cells from SARS-CoV–infected patients also prevented virus infection via WIV1-CoV spike (15, 16). Both antibodies 230.15 and 227.14 robustly inhibited WIV1-MA15 replication with kinetics similar to or exceeding SARS-CoV Urbani (Fig. 4 *B* and *C*). In contrast, antibody 109.8, which maps outside the receptor binding domain, produced only marginal neutralization of WIV1-MA15 (Fig. 4*D*). Whereas the residue associated with prior escape mutants was conserved at position 332, the adjacent residue had a significant change (K332T) in WIV1-CoV, possibly contributing to reduced efficacy of this antibody.

To further extend these findings, in vivo studies with antibody 227.14 were initiated in HFH4-ACE2–expressing mice. One day before infection, HFH4-ACE2–expressing mice were injected with 200 μg of antibody 227.14 or PBS control as previously described (17); mice were subsequently challenged with either SARS-CoV Urbani or WIV1-CoV and monitored for 7 d. The results indicate that antibody 227.14 protected mice from both lethal SARS-CoV Urbani and WIV-CoV challenge (Fig. 4*E*); in addition, lung titers revealed no detectable virus in either SARS-CoV or WIV1-CoV–infected HFH4-ACE2–expressing mouse lungs following antibody treatment (Fig. 4*F*). Together, the in vitro and in vivo data indicate that a mixture of broadly neutralizing antibodies against SARS-CoV would likely provide significant protection if WIV1-CoV–like viruses successfully transmitted to humans.

Vaccine Efficacy Limited Against WIV1 Spike. Previously, whole virion SARS-CoV inactivated by both formalin and UV irradiation (double inactivated virus, DIV) was demonstrated as a potential vaccination candidate based on robust neutralization and protection following homologous SARS-CoV challenge in young mice (18). However, both aged animal and heterologous

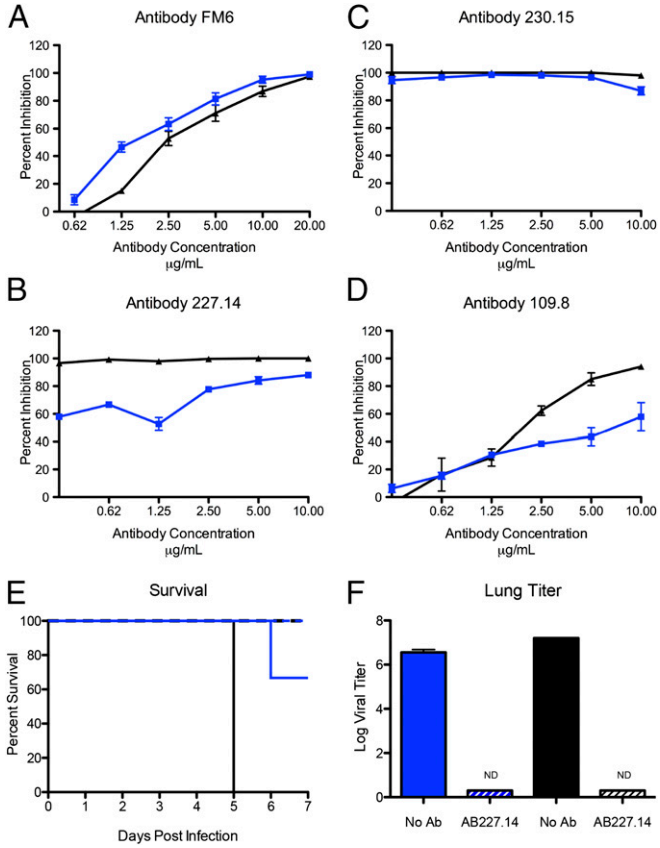

Fig. 4. SARS-CoV monoclonal antibodies have robust neutralization against WIV1 spike-mediated infection. Neutralization efficacy was evaluated using percent neutralization assays against SARS-CoV Urbani (black) or WIV1-MA15 (blue) with a panel of monoclonal antibodies: (*A*) fm6, (*B*) 230.15, (*C*) 227.15, and (*D*) 109.8, all originally generated against epidemic SARS-CoV. Each data point is representative of two or more independent neutralization wells. (*E* and *F*) Twenty- to twenty-four-week-old HFH4 ACE2-expressing mice were injected with 200 μg of anti-SARS human antibody 227.15 (hatched line) or mock (solid line) 1 d before infection with 1 × 10^5 pfu of SARS-CoV Urbani (black) or WIV1-CoV (blue) and examined over a 7-d time course for (*E*) survival ($n = 3$ for both antibody-treated groups and mock PBS control WIV1-CoV, $n = 2$ for mock-treated SARS-CoV Urbani), (*F*) day-2 lung titer ($n = 3$ for all groups). ND signifies no titers detected. For each bar graph, center value is representative of group mean and error bars are defined by SEM.

challenge studies revealed incomplete protection, increased immune pathology, and eosinophilia, indicating the possibility of adverse affects following DIV vaccination (19). To determine if heterologous challenge with WIV1-CoV spike produced a similar affect, 1-y-old BALB/c mice were vaccinated and boosted with DIV or PBS mock control. Mice were then challenged 6 wk postinitial vaccination with WIV1-MA15 and examined over a 4-d time course. Similar to previous experiments, mice infected with WIV1-MA15 had only marginal weight loss and showed no clinical signs of disease with either vaccination group (Fig. 5*A*). However, viral replication at day 4 was not significantly reduced in DIV-vaccinated groups compared with control (Fig. 5*B*). In addition, plaque reduction neutralization titers from the serum of aged DIV-vaccinated mice indicated no neutralization of WIV1-MA15, suggesting inadequate protection (Fig. 5*C*). Importantly, examination of histopathology revealed increased eosinophilia in DIV-vaccinated mice compared with PBS controls, indicating the potential for immune induced pathology due to vaccination. Together, the data indicate that DIV vaccination would not provide significant protection and may cause adverse effects in the context of WIV1-CoV spike-mediated outbreak.

Discussion

The recent outbreaks of Ebola, influenza, and MERS-CoV underscore the threat posed by viruses emerging from zoonotic sources. Coupled with air travel and uneven public health infrastructures, it is critical to develop approaches to mitigate these and future outbreaks. In this paper, we outline a platform that leverages metagenomics data, synthetic genome design, transgenic mouse models, and therapeutic human antibodies to identify and treat potential prepandemic viruses. Focusing on SARS-like CoVs, the approach indicates that viruses using the WIV1-CoV spike protein are capable of infecting HAE cultures directly without further spike adaptation. Whereas in vivo data indicate attenuation relative to SARS-CoV, the augmented replication in the presence of human *ACE2* in vivo suggests that the virus has significant pathogenic potential not captured by current small animal models. Importantly, therapeutic treatment with monoclonal antibodies suggests a Zmapp-based approach would be effective against a WIV1-CoV spike-mediated outbreak. However, failure of SARS DIV vaccine to induce protection highlights the need for continued development of additional therapeutics. Overall, the characterization of WIV1-CoV and its pathogenic potential highlight the utility of this platform in evaluating currently circulating zoonotic viruses.

Primary human airway epithelial cell cultures derived from human donors and grown at an air–liquid interface represent the

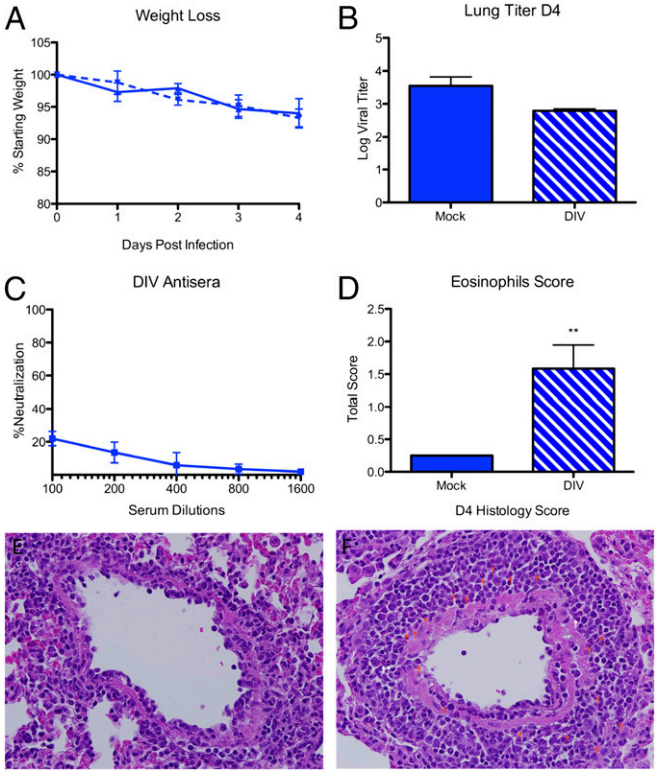

Fig. 5. Double-inactivated whole SARS-CoV vaccine fails to protect aged animals from chimeric WIV1-CoV infection. Twelve-month-old mice were vaccinated and boosted with DIV (dotted line) or PBS (solid line) and infected 21 d postboost with 10^4 pfu of WIV1-MA15 via the i.n. route. (*A*) Weight loss following WIV1-MA15 challenge and (*B*) viral replication in the lung 4 DPI. (*C*) Neutralization of WIV1-MA15 (blue) with serum from aged, DIV-vaccinated mice. (*D–H*) Histopathology lung sections stained for H&E from DIV- and mock-vaccinated mice. (*D*) Eosinophil score (scale 0–4) following DIV or mock vaccination 4 DPI. (*E* and *F*) Representative H&E lung sections for (*E*) mock- and (*F*) DIV-vaccinated mice infected with WIV-MA15. Red arrows indicate individual eosinophil locations. *P* values based on two-tailed Student's *t* test of individual time points are marked as indicated: $^{**}P < 0.01$.

closest model to the human lung. Therefore, the ability of both WIV1-CoV and WIV1-MA15 to grow equivalently to the epidemic SARS-CoV in these cultures is a major concern for emergence. However, pathogenesis studies in mice suggest that further adaptation may be required for epidemic disease. Compared with SARS equivalents, both full-length and chimeric WIV1 viruses had significant attenuation even with the presence of human *ACE2* in the mouse model. Together, the data suggest that despite using ACE2 and robust replication in primary human airway epithelial cultures, WIV1-CoV likely maintains deficits that impact pathogenesis in mice; therefore, WIV1-mediated infection may have diminished epidemic potential in humans relative to SARS-CoV.

A number of factors may contribute to reduced mouse pathogenesis observed following WIV1-CoV spike-mediated infection. In the context of both the SARS-CoV and MERS-CoV outbreaks, focus had been primarily directed to spike binding as the key component of emergence and pandemic potential. Supported by adaption at Y436H in mouse-adapted SARS spike (10), improved binding to host receptor cannot be discounted as a crucial component in emergence. This fact is supported by improved replication of WIV1-CoV in mice expressing human ACE2 compared with control (Fig. 2*D* versus Fig. 3*B*). However, in vivo attenuation of WIV1-CoV relative to SARS-CoV Urbani despite efficient infection in primary human airway cultures suggests that additional factors contribute to epidemic emergence. One possibility is that adaptation outside of spike protein may lead to emergence via altered host–virus interactions. Whereas WIV1-MA15 was attenuated relative to SARS-MA15 in vivo, overall titers in the lung were similar to the epidemic SARS-CoV Urbani in BALB/c mice (Figs. 3 and 4). These data suggest that CoV backbone changes may account for or compensate for deficits in WIV1-CoV replication compared with SARS-CoV Urbani in vivo. Another possible factor accounting for attenuation is changes to spike that are independent of receptor binding. Whereas the receptor binding domain had garnered the most interest, changes in the remaining portion of S1 as well as the S2 portion of spike may also play a critical role in facilitating CoV infection, transmission, and/or pathogenesis (20). Differences in these regions of spike may yield increased protease targeting, enhanced spike cleavage, and/or expanded tropism leading to more robust infection for the epidemic SARS strains. Globally, the in vivo results suggest that any of these areas may have contributed to SARS-CoV emergence. However, even these interpretations must be tempered due to the robust differences between mouse and human models; further studies in nonhuman primates are required to confirm these results and derive further insight into CoV emergence from zoonotic sources.

Despite the differences in the backbone genome sequences, therapeutics developed against SARS-CoV provide some measure of protection in the context of a future outbreak. Testing the four most broadly neutralizing SARS-CoV antibodies revealed effective control of WIV1-MA15 at relatively low concentrations of antibody (14, 15, 21). For two of the four antibodies tested (Fm6 and 230.15), WIV1-CoV spike-expressing virus was neutralized equivalently or better than SARS-CoV Urbani. Similarly, only minimal differences at the low end of the neutralization curve were noted for antibody 227.14. Whereas antibody 109.8 produced only marginal neutralization of WIV1-MA15, the overall antibody neutralization data argue that multivalent monoclonal antibody approaches could limit a WIV1-CoV spike-mediated outbreak. As such, a "ZMapp"-based approach could have great potential in stemming or preventing a future SARS-CoV–like outbreak.

In contrast to the success of monoclonal antibodies, vaccine failure indicated further development and refinement are necessary. The development of a DIV SARS-CoV vaccine was buoyed as a possible means to control SARS-CoV outbreaks based on robust neutralization and protection in young mice (18). However, studies with DIV in aged animals revealed incomplete protection, significant immune pathology, and eosinophilia (19). Despite these prior results, the efficacy of monoclonal antibody treatments made further testing of DIV seemingly worthwhile against WIV1-CoV spike-mediated infection. However, the results remained the same, as vaccination of aged mice resulted in no protection from WIV1-MA15 replication in vivo (Fig. 5). Importantly, increased immune pathology and observed eosinophilia indicate that broad-based vaccination efforts against SARS-CoV–like viruses must consider heterologous viruses as well as failure due to senescence in the aged host. A number of novel platforms including Venezuelan Equine Encephalitis Virus Replicon Particle (VRP) and live-attenuated vaccine approaches show great promise in these areas, but require further testing and development before deployment in an outbreak setting (22, 23).

Overall, the results from these studies highlight the utility of a platform that leverages metagenomics findings and reverse genetics to identify prepandemic threats. For SARS-like WIV1-CoV, the data can inform surveillance programs, improve diagnostic reagents, and facilitate effective treatments to mitigate future emergence events. However, building new and chimeric reagents must be carefully weighed against potential gain-of-function (GOF) concerns. Whereas not generally expected to increase pathogenicity, studies that build reagents based on viruses from animal sources cannot exclude the possibility of increased virulence or altered immunogenicity that promote escape from current countermeasures. As such, the potential of a threat, real or perceived, may cause similar exploratory studies to be limited out of an "abundance of caution." Importantly, the government pause on GOF studies may have already impacted the scope and direction of these studies. Whereas previous adaption of the epidemic SARS-CoV strain provided insights into species-specific changes, bat-derived WIV1 adaptation may identify elements critical for pathogenesis and transition from reservoir to human host; targets include viral proteins that interact with host machinery or host immunity like NSP1, envelope, or ORF6 (22, 24, 25). Similarly, WIV1-CoV could be used to drive improved therapeutics, including escape mutants for improved monoclonal antibodies or more broadly neutralizing vaccine approaches. However, it remains unclear from the current policies and GOF environment if these types of studies will be permissible. Although limits and standards for these types of experiments must be established, erring on the side of caution is not without its own risks and balancing the benefits of these types of studies must also be weighed against the potential hazards.

Using a novel platform to translate metagenomics findings, the WIV1-CoV cluster has been identified as a threat for future emergence in human populations due to robust replication in primary human airway epithelial cell cultures. However, based on in vivo mouse data, additional adaptations will likely be required to produce epidemic disease. Notably, whereas current antibody-based therapies hold great promise in treating WIV1-CoV spike-mediated infection, failure of SARS-CoV vaccination approaches presents a major challenge for any efforts to protect against future emergent viruses. Together, the data illustrate the utility of the platform and highlight the need to build and maintain preparations for future emergence events.

Materials and Methods

Viruses, Cells, and Infection. Wild-type and chimeric CoVs were cultured on Vero E6 cells, grown in DMEM (Gibco) and 5% fetal clone serum (HyClone) along with anti/anti (Gibco). Growth curves in Vero and primary human airway epithelial cells were performed as previously described (26, 27). Human lungs were procured under University of North Carolina at Chapel Hill (UNC) Institutional Review Board-approved protocols.

Construction of Chimeric SARS-Like Viruses. Both wild-type and chimeric WIV-CoV infectious clones were designed using published sequences and based on the SARS-CoV infectious clone (10). Synthetic construction of chimeric mutant and full-length WIV1-CoV were approved by the UNC Institutional Biosafety Committee and the Dual Use Research of Concern Committee.

Ethics Statement. The study was carried out in accordance with the recommendations for care and use of animals by the Office of Laboratory Animal Welfare (OLAW), National Institutes of Health. The Institutional Animal Care and Use Committee (IACUC) of University of North Carolina (UNC permit no. A-3410-01) approved the animal study protocol (IACUC no. 13–033).

Mice and in Vivo Infection. Female 10-wk- and 12-mo-old Balb/cAnNHsD mice ordered from the Harlan Labs were infected as previously described (23). For vaccination, young and aged mice were vaccinated and boosted by footpad injection with a 20-μL volume of either 0.2 μg of double-inactivated SARS-CoV vaccine (DIV) with alum or mock PBS as previously described (19).

Generation and Infection of ACE2 Tissue-Specific Transgenic Mice. Transgenic mice with airway-targeted overexpression of human *ACE2* were generated by microinjection of fertilized C3H × C57BL/6 (C3B6) F_1 hybrid oocytes with an expression cassette consisting of the HFH4/FOXJ1 lung ciliated epithelial cell-specific promoter elements and the coding region of *ACE2* cDNA in a pTG1 vector (11) (UNC Animal Model Core). Founder mice were crossed to C3B6, producing human ACE2-transgenic mice that were each previously tested for transgene expression as described in *SI Materials and Methods*. ACE2-transgenic mice given i.p. injection of 200 μg of human Ab S227.14 or PBS control (0.20 mL total volume, five to six mice per group) 1 d before infection as previously described (17).

Histological Analysis. Lung tissues for histological analysis were fixed in buffered formalin phosphate 10% (4–5% wt/wt formaldehyde) (Fisher #SF100-20) for at least 7 d, tissues were embedded in paraffin, and 5-μm sections were prepared by the UNC histopathology core facility as previous described (23). Images were captured using an Olympus BX41 microscope with an Olympus DP71 camera.

Virus Neutralization Assays. Plaque reduction neutralization titer assays were preformed with previously characterized antibodies against SARS-CoV as previously described (14, 15, 21). Briefly, neutralizing antibodies or serum were serially diluted twofold and incubated with 100 pfu of the different virus strains for 1 h at 37 °C. The virus and antibodies were then added to a six-well plate with 5×10^5 Vero E6 cells per well with $n \geq 2$. After a 1-h incubation at 37 °C, cells were overlaid with 3 mL of 0.8% agarose in media. Plates were incubated for 2 d at 37 °C and then stained with neutral red for 3 h, and plaques were counted. The percentage of plaque reduction was calculated as [1 − (no. of plaques with antibody/no. of plaques without antibody)] × 100.

Statistical Analysis. All experiments were conducted contrasting two experimental groups (either two viruses or vaccinated and unvaccinated cohorts). Therefore, significant differences in viral titer and histology scoring were determined by a two-tailed Student's *t* test at individual time points. Data were normally distributed in each group being compared and had similar variance.

Biosafety and Biosecurity. Reported studies were initiated after the University of North Carolina Institutional Biosafety Committee approved the experimental protocol: project title: Generating infectious clones of Bat SARS-like CoVs; lab safety plan ID: 20145741; schedule G ID: 12279. These studies were initiated before the US Government Deliberative Process Research Funding Pause on Selected Gain of Function Research Involving Influenza, MERS, and SARS Viruses (www.phe.gov/s3/dualuse/Documents/gain-of-function.pdf), and the current paper has been reviewed by the funding agency, the National Institutes of Health (NIH). Continuation of these studies has been requested and approved by the NIH.

ACKNOWLEDGMENTS. We thank Dr. Zhengli-Li Shi of the Wuhan Institute of Virology for access to bat CoV sequences and plasmid of WIV1-CoV spike protein. Research was supported by the National Institute of Allergy and Infectious Disease and the National Institute of Aging of the NIH under Awards U19AI109761 and U19AI107810 (to R.S.B.), AI1085524 (to W.A.M.), and F32AI102561 and K99AG049092 (to V.D.M.). Human airway epithelial cell cultures were supported by the National Institute of Diabetes and Digestive and Kidney Disease under Award NIH DK065988 (to S.H.R.). Support for the generation of the mice expressing human ACE2 was provided by NIH Grants AI076159 and AI079521 (to A.C.S.).

1. Peiris JS, Guan Y, Yuen KY (2004) Severe acute respiratory syndrome. *Nat Med* 10(12, Suppl):S88–S97.
2. Al-Tawfiq JA, et al. (2014) Surveillance for emerging respiratory viruses. *Lancet Infect Dis* 14(10):992–1000.
3. Graham RL, Baric RS (2010) Recombination, reservoirs, and the modular spike: Mechanisms of coronavirus cross-species transmission. *J Virol* 84(7):3134–3146.
4. Graham RL, Donaldson EF, Baric RS (2013) A decade after SARS: Strategies for controlling emerging coronaviruses. *Nat Rev Microbiol* 11(12):836–848.
5. Ge XY, et al. (2013) Isolation and characterization of a bat SARS-like coronavirus that uses the ACE2 receptor. *Nature* 503(7477):535–538.
6. He B, et al. (2014) Identification of diverse alphacoronaviruses and genomic characterization of a novel severe acute respiratory syndrome-like coronavirus from bats in China. *J Virol* 88(12):7070–7082.
7. Yount B, et al. (2003) Reverse genetics with a full-length infectious cDNA of severe acute respiratory syndrome coronavirus. *Proc Natl Acad Sci USA* 100(22):12995–13000.
8. Frieman M, et al. (2012) Molecular determinants of severe acute respiratory syndrome coronavirus pathogenesis and virulence in young and aged mouse models of human disease. *J Virol* 86(2):884–897.
9. Gillim-Ross L, et al. (2004) Discovery of novel human and animal cells infected by the severe acute respiratory syndrome coronavirus by replication-specific multiplex reverse transcription-PCR. *J Clin Microbiol* 42(7):3196–3206.
10. Roberts A, et al. (2007) A mouse-adapted SARS-coronavirus causes disease and mortality in BALB/c mice. *PLoS Pathog* 3(1):e5.
11. Ostrowski LE, Hutchins JR, Zakel K, O'Neal WK (2003) Targeting expression of a transgene to the airway surface epithelium using a ciliated cell-specific promoter. *Mol Ther* 8(4):637–645.
12. Netland J, Meyerholz DK, Moore S, Cassell M, Perlman S (2008) Severe acute respiratory syndrome coronavirus infection causes neuronal death in the absence of encephalitis in mice transgenic for human ACE2. *J Virol* 82(15):7264–7275.
13. Qiu X, et al. (2014) Reversion of advanced Ebola virus disease in nonhuman primates with ZMapp. *Nature* 514(7520):47–53.
14. Sui J, et al. (2008) Broadening of neutralization activity to directly block a dominant antibody-driven SARS-coronavirus evolution pathway. *PLoS Pathog* 4(11):e1000197.
15. Rockx B, et al. (2010) Escape from human monoclonal antibody neutralization affects in vitro and in vivo fitness of severe acute respiratory syndrome coronavirus. *J Infect Dis* 201(6):946–955.
16. Traggiai E, et al. (2004) An efficient method to make human monoclonal antibodies from memory B cells: Potent neutralization of SARS coronavirus. *Nat Med* 10(8):871–875.
17. Zhu Z, et al. (2007) Potent cross-reactive neutralization of SARS coronavirus isolates by human monoclonal antibodies. *Proc Natl Acad Sci USA* 104(29):12123–12128.
18. Spruth M, et al. (2006) A double-inactivated whole virus candidate SARS coronavirus vaccine stimulates neutralising and protective antibody responses. *Vaccine* 24(5):652–661.
19. Bolles M, et al. (2011) A double-inactivated severe acute respiratory syndrome coronavirus vaccine provides incomplete protection in mice and induces increased eosinophilic proinflammatory pulmonary response upon challenge. *J Virol* 85(23):12201–12215.
20. McRoy WC, Baric RS (2008) Amino acid substitutions in the S2 subunit of mouse hepatitis virus variant V51 encode determinants of host range expansion. *J Virol* 82(3):1414–1424.
21. Sui J, et al. (2014) Effects of human anti-spike protein receptor binding domain antibodies on severe acute respiratory syndrome coronavirus neutralization escape and fitness. *J Virol* 88(23):13769–13780.
22. DeDiego ML, et al. (2014) Coronavirus virulence genes with main focus on SARS-CoV envelope gene. *Virus Res* 194:124–137.
23. Agnihothram S, et al. (2014) A mouse model for Betacoronavirus subgroup 2c using a bat coronavirus strain HKU5 variant. *MBio* 5(2):e00047–e14.
24. Narayanan K, Ramirez SI, Lokugamage KG, Makino S (2015) Coronavirus nonstructural protein 1: Common and distinct functions in the regulation of host and viral gene expression. *Virus Res* 202:89–100.
25. Bolles M, Donaldson E, Baric R (2011) SARS-CoV and emergent coronaviruses: Viral determinants of interspecies transmission. *Curr Opin Virol* 1(6):624–634.
26. Sheahan T, Rockx B, Donaldson E, Corti D, Baric R (2008) Pathways of cross-species transmission of synthetically reconstructed zoonotic severe acute respiratory syndrome coronavirus. *J Virol* 82(17):8721–8732.
27. Sims AC, et al. (2013) Release of severe acute respiratory syndrome coronavirus nuclear import block enhances host transcription in human lung cells. *J Virol* 87(7):3885–3902.